Governing Equation Identification of Nonlinear Single Degree-of-Freedom Oscillators With Coulomb Friction Using Explicit Stick and Slip Temporal Constraints

Mahajan, Saurabh; Cicirello, Alice

DOI
10.1115/1.4063070

Publication date
2023

Document Version
Final published version

Published in
ASCE-ASME Journal of Risk and Uncertainty in Engineering Systems, Part B: Mechanical Engineering

Citation (APA)
Mahajan, S., & Cicirello, A. (2023). Governing Equation Identification of Nonlinear Single Degree-of-Freedom Oscillators With Coulomb Friction Using Explicit Stick and Slip Temporal Constraints. *ASCE-ASME Journal of Risk and Uncertainty in Engineering Systems, Part B: Mechanical Engineering*, *9*(4), Article 041101. https://doi.org/10.1115/1.4063070

ASCE-ASME Journal of Risk and Uncertainty in Engineering Systems Part B: Mechanical Engineering
Online journal at:
asmedigitalcollection.asme.org/risk

Governing Equation Identification of Nonlinear Single Degree-of-Freedom Oscillators With Coulomb Friction Using Explicit Stick and Slip Temporal Constraints

Saurabh Mahajan
Faculty of Civil Engineering and Geosciences,
Delft University of Technology,
South Holland, Delft 2628 CN, Netherlands
e-mail: s.r.mahajan@student.tudelft.nl

Alice Cicirello
Faculty of Civil Engineering and Geosciences,
Delft University of Technology,
South Holland, Delft 2628 CN, Netherlands
e-mail: A.Cicirello@tudelft.nl

The friction force at joints of engineering structures is usually unknown and not directly identifiable. This contribution explores a procedure for obtaining the governing equation of motion and correctly identifying the unknown Coulomb friction force of a mass-spring-dashpot system. In particular, a single degree-of-freedom system is investigated both numerically and experimentally. The proposed procedure extends the state-of-the-art data-driven sparse identification of nonlinear dynamics (SINDy) algorithm by developing a methodology that explicitly imposes constraints encoding knowledge of the nonsmooth dynamics experienced during stick-slip phenomena. The proposed algorithm consists of three steps: (i) data segregation of mass-motion from mass-sticking during stick-slip response; (ii) application of SINDy on the mass-motion dataset to obtain the functional form of the governing equation; and (iii) applying sticking and slipping conditions to identify the unknown system parameters. It is shown that the proposed approach yields an improved estimate of the uncertain system parameters such as stiffness, viscous damping, and magnitude of friction force (all mass normalized) for various signal-to-noise ratios compared to SINDy. [DOI: 10.1115/1.4063070]

Keywords: stick and slip temporal constraints, nonlinear dynamic system identification, SINDy, epistemic uncertainty, discontinuous nonlinearity, Coulomb friction

1 Introduction

The dynamics of various engineering structures like wind turbines, robots, buildings, etc., are greatly influenced by the friction present in joints. The amplitude of structural response can be drastically reduced due to the loss of energy resulting from frictional contact. As a result of heat produced because of friction, repetitive motion can cause wear and tear of the surfaces in contact with each other. Hence, it is important to identify the functional form of the friction force contributing to the dynamic behavior of engineering systems as it would improve models employed for predicting the response of structures in operating conditions. Currently, it is not possible to directly characterize the friction force of structural joints without affecting the joint behavior itself. Consequently, the friction force can be regarded as an epistemic uncertainty that is uncertainty caused by lack of knowledge. To this end, a large body of research has focused on the use and development of system identification approaches which use measurements of output and input signals to a dynamic system. These approaches can be broadly grouped as follows: (i) approaches based on an equivalent linearization techniques as well as stochastic linearization methods [1–5]; (ii) time-domain methods, such as auto-regressive with eXogenous input model (ARX) for linear systems [1,6,7] and nonlinear auto-regressive with eXogenous (NARX), nonlinear auto-regressive moving-average with exogenous inputs model (NARMAX) for nonlinear system identification [8]. However, the NARX model fails to capture the noise as a separate entity, which is overcome by NARMAX. NARMAX models the nonlinearity as a polynomial function, which might limit its applicability. The final approach (iii) leverages Machine Learning strategies because of the availability of measurement of the external excitation and response of nonlinear systems. The last group has recently gained particular interest in the research community [9]. The sparse identification of nonlinear dynamics (SINDy) [10–12] belongs to this group and has recently been applied to estimate the governing equation of motion (EOM) based on the data of input and output of a dynamic system. SINDy has been applied for identifying EOM in the chemical reactor [13], parameters of the power grid model [14], and delayed differential equation [15]. In particular, in nonlinear structural dynamics, it has been used for estimating nonlinear normal modes [16], and reconstructing governing EOM for geometrical nonlinear systems [17]. However, in the presence of a discontinuous nonlinearity, e.g., frictional joints subject to the stick-slip motion, the error in

Manuscript received April 20, 2023; final manuscript received July 27, 2023; published online August 25, 2023. Assoc. Editor: Jie Yuan.

predictions of the SINDy algorithm can be substantial, as shown in this paper. This leads to errors in the estimates of the epistemic uncertain system parameters, such as stiffness, viscous damping, and value of nonlinear force in a dynamic system (all mass normalized), which are fixed but unknown.

To address this issue for a single degree-of-freedom (SDOF) system with Coulomb friction subject to a harmonic excitation, the extended SINDy is proposed by introducing two key modifications to SINDy [10]. First, in the stick-slip dynamic regime, the data of response and forcing is segregated into mass-sticking and mass-motion. Further the data of mass-motion is used as an input for the existing SINDy algorithm to identify the correct functional form of EOM. Second, the correct functional form of the EOM is used to enforce the physics-based constraints to estimate the epistemic uncertain system parameters. The applicability and accuracy of the extended SINDy algorithm for obtaining the EOM are explored and compared to SINDy, also in the presence of varying noise levels.

2 Sparse Identification of Nonlinear Dynamics Algorithm: Review and Applicability

2.1 Review. Let us consider a dynamic system whose governing equations can be written as [10]

$$\frac{d}{dt}\boldsymbol{x}(t) = \boldsymbol{f}(\boldsymbol{x}(t)) \tag{1}$$

where $\boldsymbol{x}(t)$ is the state vector with n number of states of the system at general time instant t ($\boldsymbol{x}(t) = [x_1(t), x_2(t), \ldots, x_n(t)]^T$) and $\boldsymbol{f}(\boldsymbol{x}(t))$ is a vector that represents the dynamic system in terms of mass, stiffness, viscous damping and nonlinear forces present in the system. By explicitly accounting for an external forcing $\boldsymbol{u}(t)$, Eq. (1) can be rewritten as [10]

$$\frac{d}{dt}\boldsymbol{x}(t) = \boldsymbol{f}(\boldsymbol{x}(t), \boldsymbol{u}(t)) \tag{2}$$

The system's response ($\boldsymbol{X}$) to the forcing ($\boldsymbol{U}$) can be written in a matrix form to account for the N discrete time steps as [10]

$$\boldsymbol{X} = \begin{bmatrix} \boldsymbol{x}^T(t_1) \\ \boldsymbol{x}^T(t_2) \\ \vdots \\ \boldsymbol{x}^T(t_N) \end{bmatrix} = \begin{bmatrix} x_1(t_1) & x_2(t_1) & \cdots & x_n(t_1) \\ x_1(t_2) & x_2(t_2) & \cdots & x_n(t_2) \\ \vdots & \vdots & \ddots & \vdots \\ x_1(t_N) & x_2(t_N) & \ldots & x_n(t_N) \end{bmatrix} \tag{3}$$

$$\boldsymbol{U} = \begin{bmatrix} \boldsymbol{u}^T(t_1) \\ \boldsymbol{u}^T(t_2) \\ \vdots \\ \boldsymbol{u}^T(t_N) \end{bmatrix} = \begin{bmatrix} u_1(t_1) & u_2(t_1) & \cdots & u_n(t_1) \\ u_1(t_2) & u_2(t_2) & \cdots & u_n(t_2) \\ \vdots & \vdots & \ddots & \vdots \\ u_1(t_N) & u_2(t_N) & \ldots & u_n(t_N) \end{bmatrix} \tag{4}$$

$$\dot{\boldsymbol{X}} = \begin{bmatrix} \dot{\boldsymbol{x}}^T(t_1) \\ \dot{\boldsymbol{x}}^T(t_2) \\ \vdots \\ \dot{\boldsymbol{x}}^T(t_N) \end{bmatrix} = \begin{bmatrix} \dot{x}_1(t_1) & \dot{x}_2(t_1) & \cdots & \dot{x}_n(t_1) \\ \dot{x}_1(t_2) & \dot{x}_2(t_2) & \cdots & \dot{x}_n(t_2) \\ \vdots & \vdots & \ddots & \vdots \\ \dot{x}_1(t_N) & \dot{x}_2(t_N) & \ldots & \dot{x}_n(t_N) \end{bmatrix} \tag{5}$$

Hence, the final form of the governing equation of dynamic system is written in a standard state-space formulation as [18]

$$\dot{\boldsymbol{X}} = \boldsymbol{A}\boldsymbol{X} + \boldsymbol{B}\boldsymbol{U} \tag{6}$$

where $\boldsymbol{A}$ and $\boldsymbol{B}$ are the state and input matrix, respectively. SINDy [10] identifies the unknown governing EOM from the available data of external forcing and of the response to external forcing. The identification is performed using sparsity promoting techniques and machine learning. Some user-specified set of functions which might be contributing to describe the governing EOM of the dynamic system are listed (e.g., see Eq. (7)). A sparse regression with low risk of overfitting is obtained by the combination of sparsity and user-specified terms, producing a parsimonious model [10]. The user-specified terms are included in the candidate function library $\boldsymbol{\Theta}(\boldsymbol{X})$ which might contain polynomial terms, trigonometric terms, exponential terms and other user-specified functions (e.g., g($\mathbf{X}$)), or their combination [10]. For example

$$\boldsymbol{\Theta}(\boldsymbol{X}) = \left[\boldsymbol{I}\,\boldsymbol{X}\,\boldsymbol{X}^{\boldsymbol{P2}}\,\boldsymbol{X}^{\boldsymbol{P3}}\ldots \sin(\boldsymbol{X})\cos(\boldsymbol{X})\; e^{\boldsymbol{X}} g(\boldsymbol{X})\ldots\right] \tag{7}$$

where the $N \times n$ matrix representing ith order polynomial terms is

$$\boldsymbol{X}^{\boldsymbol{Pi}} = \begin{bmatrix} {x_1}^i(t_1) & {x_2}^i(t_1) & \cdots & {x_n}^i(t_1) \\ {x_1}^i(t_2) & {x_2}^i(t_2) & \cdots & {x_n}^i(t_2) \\ \vdots & \vdots & \ddots & \vdots \\ {x_1}^i(t_N) & {x_2}^i(t_N) & \ldots & {x_n}^i(t_N) \end{bmatrix} \tag{8}$$

A selection matrix $\boldsymbol{\Xi} = [\xi_1 \xi_2\, \xi_3\, .\xi_n]$ is then introduced, such that the final equation in the state-space form is written as [10]

$$\dot{\boldsymbol{X}} = \boldsymbol{\Theta}(\boldsymbol{X})\boldsymbol{\Xi} \tag{9}$$

The selection matrix $\boldsymbol{\Xi}$ selects the terms in Eq. (7) that will be present in the governing EOM [10]. This is done by introducing an optimizer with specific minimization function [10]. For example, if the Sequential Threshold Least Squares (STLSq) is used, the minimization function is given by [10]

$$\|\dot{\boldsymbol{X}} - \boldsymbol{\Theta}(\boldsymbol{X})\boldsymbol{\Xi}\|_2^2 + \alpha\|\boldsymbol{\Xi}\|_2^2 \tag{10}$$

where α is a coefficient that is chosen by the user to boost the sparsity of the terms in the governing EOM. A high value of α leads to a smaller number of terms in the governing EOM.

2.2 Applicability of Sparse Identification of Nonlinear Dynamics to Friction Problems. Although never explicitly mentioned in the literature, the applicability of the SINDy algorithm [10] depends on the functional form of the governing EOM. The dynamic system might contain a nonlinear restoring force term, which is discontinuous or changes abruptly in the time domain leading to a nonsmooth response. The nonsmooth response is a response where the dynamic system changes abruptly from one motion regime to another in the time domain. For example, when the restoring force is a function of signum as in the case of the Coulomb friction model, the response of a SDOF dynamic system with such friction model can be characterized by a sequence of mass-motion and mass-sticking regimes. The EOM representing such a dynamic system is stiff [19]. Without any specified constraints, SINDy performs a regression poorly on such a sequence of regimes to estimate an EOM that would fit simultaneously both mass-motion and mass-sticking. As a major part of the regime consists of mass-motion, the SINDy algorithm would identify the correct functional form of the EOM. However, the coefficients of the identified EOM would be inaccurate.

Let us consider a SDOF dynamic system with friction subject to a harmonic excitation $u(t) = A\sin(\omega t)$ (where A and ω denote the amplitude and frequency of harmonic base excitation, respectively), as shown in Fig. 1(*a*), and described by

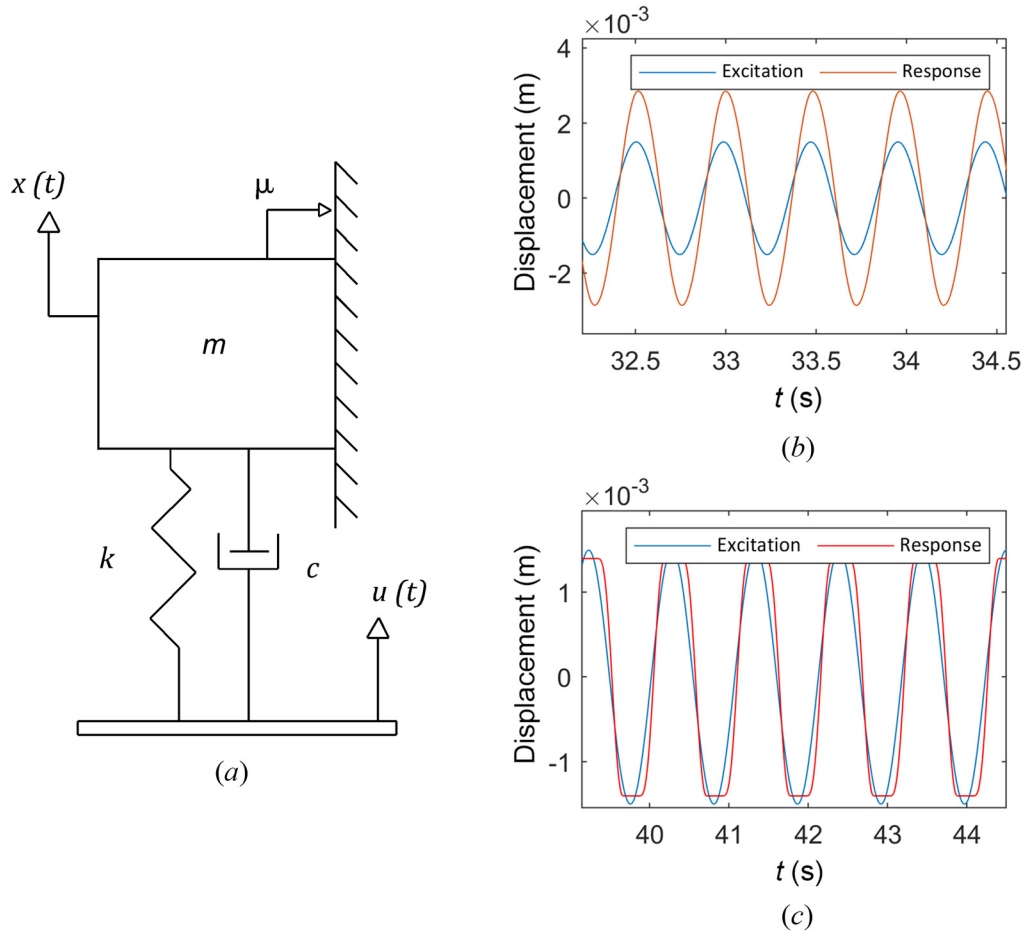

Fig. 1 Schematic representation of SDOF with friction (*a*), response of SDOF in continuous motion (*b*) and stick-slip motion (*c*)

$$m\ddot{x}(t) + c\dot{x}(t) + kx(t) + F_f sgn[\dot{x}(t)] = ku(t) + c\dot{u}(t) \tag{11}$$

where k, c, m, F_f, $x(t)$, and $u(t)$ are the stiffness, viscous damping, mass, friction force magnitude, displacement of SDOF, and harmonic base excitation, respectively, all represented in SI units.

The magnitude of friction force (F_f) is defined as a product of the coefficient of friction (μ) and the normal force exerted by mass on the surface. The function sgn[.] represents signum function. The EOM of such a system can be represented in a state-space form as

$$\begin{cases} x_1(t) = x(t) \\ \begin{bmatrix} \dot{x}_1(t) \\ \dot{x}_2(t) \end{bmatrix} = \begin{bmatrix} 0 & 1 \\ -\hat{k} & -\hat{c} \end{bmatrix} \begin{bmatrix} x_1(t) \\ x_2(t) \end{bmatrix} + \begin{bmatrix} 0 \\ -\hat{F}_f \text{sgn}[\dot{x}(t)] \end{bmatrix} \\ \quad + \begin{bmatrix} 0 \\ \hat{k}u(t) + \hat{c}\dot{u}(t) \end{bmatrix} \forall x_2 \neq 0 \end{cases} \tag{12}$$

where $\hat{k}$, $\hat{c}$, $\hat{F}_f$, $x_2(t)$ are the mass-normalized stiffness, viscous damping, friction force magnitude, velocity of SDOF, respectively (see Table 1).

It is worth mentioning that the synthetic data is obtained by numerically solving Eq. (12) with ode45 function in MATLAB [20] and explicitly setting the event conditions as explained in Ref. [19] for dealing with stiff problems. The event conditions are [21]

$$\left|\hat{c}\dot{u}(\boldsymbol{t}) + \hat{k}u(\boldsymbol{t}) - \hat{k}x_1(\boldsymbol{t})\right| \leq \widehat{F}_f \boldsymbol{I} \tag{13}$$

$$\left|\hat{c}\dot{u}(\boldsymbol{t}) + \hat{k}u(\boldsymbol{t}) - \hat{k}x_1(\boldsymbol{t}) - \dot{x}_2(\boldsymbol{t}) - \hat{c}x_2(\boldsymbol{t})\right| \geq \widehat{F}_f \boldsymbol{I} \tag{14}$$

where $|.|$ denotes absolute value, $\boldsymbol{t}$ is a vector representing different time instants $\boldsymbol{t} = \begin{bmatrix} t_1 & t_2 & \dots & t_N \end{bmatrix}^T$, and $\boldsymbol{I}$ denotes a vector with all entries as 1, respectively. The physical meaning of Eq. (13) is that the mass will indefinitely remain still until Eq. (13) is satisfied [21]. Further, the mass will remain in motion until Eq. (14) is satisfied. This can be further interpreted as follows [21]: when the velocity is zero and the mass is sticking, the friction force is sufficient to resist the inertial force, spring force, and viscous damping force—as described by Eq. (13); when the velocity is nonzero, the friction force is insufficient to resist the restoring forces as described by Eq. (14). This mass-sticking and mass-motion phenomenon cannot be accurately represented by solving Eq. (12) numerically. Hence, the event conditions are explicitly enforced.

Further, $x_1(t)$ and $x_2(t)$ represent the displacement and velocity of SDOF dynamic system in continuous time domain. To perform the analysis in discrete time domain, the displacement and velocity are represented as vectors $x_1(\boldsymbol{t})$ and $x_2(\boldsymbol{t})$. $\dot{x}_2(\boldsymbol{t})$ is obtained by numerically differentiating $x_2(\boldsymbol{t})$. In this paper, the smooth finite

Table 1 Properties of synthetic as well as experimental dynamic system

Quantity	Description	Value	Units
$\hat{k}$	Mass normalized stiffness	358.706	$\frac{N}{\text{m} \cdot \text{kg}}$
$\hat{c}$	Mass normalized viscous damping	0.0658	$\frac{Ns}{\text{m} \cdot \text{kg}}$
$\widehat{F_f}$	Mass normalized magnitude of friction force	0.0856	$\frac{N}{\text{kg}}$

Table 2 Base excitation frequencies for synthetic and experimental case study

	Base excitation frequencies (Hz)		
	Continuous motion	Two-stop stick-slip motion	Four-stop stick-slip motion
Synthetic case study	2.013, 2.583, 4.611	0.95, 1.034, 1.11	0.47, 0.51, 0.54
Experimental case study	2.013, 2.583, 4.611	1.023, 1.07, 1.10	0.61, 0.62, 0.64

Table 3 Results of system identification using synthetically generated data

Regime	Algorithm	Identified equation	RMSE (10^{-4}m)
Continuous motion	SINDy	$\dot{x_1} = x_2$ $\dot{x_2} = -358.706x_1 - 0.08x_2 + 358.432u + 0.08\dot{u} - 0.085\text{sgn}(x_2)$	0.014
	Extended SINDy	Converges to SINDy	—
Two-stop stick-slip motion	SINDy	$\dot{x_1} = 0.97x_2$ $\dot{x_2} = -336.48x_1 - 0.47x_2 + 332.5u + 1.2\dot{u} - 0.015\text{sgn}(x_2)$	1.06
	Extended SINDy	$\dot{x_1} = 0.97x_2$ $\dot{x_2} = -355.69x_1 - 0.05x_2 + 355.69u + 0.05\dot{u} - 0.08\text{sgn}(x_2)$	0.01
Four-stop stick-slip motion	SINDy	$\dot{x_1} = 0.97x_2$ $\dot{x_2} = -323.482x_1 - 0.41x_2 + 369.92u + 1.5\dot{u} - 0.025\text{sgn}(x_2)$	5.4
	Extended SINDy	$\dot{x_1} = 0.97x_2$ $\dot{x_2} = -354.56x_1 - 0.04x_2 + 354.56u + 0.04\dot{u} - 0.083\text{sgn}(x_2)$	0.05

differentiation available in Python package for SINDy (PySINDy) package is used for performing the numerical differentiation. In particular, the Savitzky–Golay filter is used in smooth finite differentiation. The window length specified in smooth finite differentiation governs the accuracy of the differentiation. The base is excited at different excitation frequencies (see Table 2) to investigate the response of the mass in continuous, two-stop stick-slip, and four-stop stick-slip regime. The continuous and the stick-slip motion of the SDOF system shown in Figs. 1(*b*) and 1(*c*) are obtained for the values of system parameters specified in Table 1.

From external excitation and response data, the SINDy [10] is applied to estimate the governing EOM in state-space form. The nonlinear system identification is done in the PySINDy [11]. PySINDy includes a candidate library and an optimizer for performing regression analysis on the collected data. The custom library chosen for the problem at hand includes linear polynomial and signum functions. For the regression analysis, the sequential threshold least squares (STLSq) and sparse relaxed regularized regression (SR3) [22] optimizer are selected for continuous and stick–slip motion, respectively. The threshold values of 0.01 and 0.05 are used for STLSq and SR3, respectively. SR3 optimizer is used with the constraint $\frac{dx_1(t)}{dt} = x_2(t)$. Further, the SINDy is used to obtain the governing EOM as shown in Table 3.

As anticipated, it is observed from Fig. 2 that the SINDy algorithm estimates the governing EOM with good accuracy in the case of continuous motion. However, from Table 3, it is observed that SINDy [10] fails to identify the coefficients of the EOM correctly in the case of two-stop and four-stop stick-slip motion. Based on this physics understanding of the problem, it is clear that there is a need to incorporate explicitly the stick and slip temporal constraints stated in Eqs. (13) and (14).

3 Extended Sparse Identification of Nonlinear Dynamics

The extended SINDy is an approach proposed to address the identification of the governing equation of the SDOF system with Coulomb friction, and it is generally applicable to the dynamic system with discontinuous restoring force when the physics constraints in the time domain are known along with the measurements of the input and output of such system. The main idea behind the extended SINDy is to augment the pre-existing SINDy algorithm by explicitly enforcing the physics constraints in the time domain by means of a three-step procedure. The detailed step-by-step procedure is described in Secs. 3.1–3.3.

3.1 Step 1: Data Segregation. Consider a SDOF system with Coulomb friction system subject to a harmonic excitation described by Eq. (12). In the stick–slip regime, the motion is a combination of mass-motion and mass-sticking. To obtain a correct functional form of the EOM, the data points of mass-motion and mass-sticking are stored separately. The segregation is done based on the condition applied to the velocity at each time instant as

$$\begin{cases} |x_2(\boldsymbol{t})| \le v_{\text{stop}} \rightarrow t\epsilon\boldsymbol{t}_{\text{stop}} \rightarrow \boldsymbol{x}_{\text{stop}} = x(\boldsymbol{t}_{\text{stop}}) \\ |x_2(\boldsymbol{t})| > v_{\text{slip}} \rightarrow t\epsilon\boldsymbol{t}_{\text{slip}} \rightarrow \boldsymbol{x}_{\text{slip}} = x(\boldsymbol{t}_{\text{slip}}) \end{cases} \tag{15}$$

where v_{stop} and v_{slip} denote the cutoff velocity for mass-stop and mass-motion, respectively. These values are specified by the user and are based on the available measurements of the velocity. The v_{stop} will strongly depend on the noise level in the measurements and will be chosen such that $v_{\text{stop}} \sim 0$. As a rule of thumb, v_{slip} is chosen such that $v_{\text{slip}} \gg v_{\text{stop}}$ and $v_{\text{slip}} \approx \max\left(\frac{|x_2(t)|}{20}\right)$.

3.2 Step 2: Using Python Package for Sparse Identification of Nonlinear Dynamics. The data points of mass-motion are used as an input to the SINDy [10] algorithm implemented in PySINDy [11], and the functional form of the EOM is identified. The steps within SINDy have been already described in Sec. 2.1. The computational cost of this step is equivalent to that of using SINDy. By implementing the STLSq and SR3, the number of iterations needed to converge to a sparse solution is drastically reduced when compared to the LASSO [10].

3.3 Step 3: Adding Constraints on Mass-Sticking and Mass-Motion Datasets. In this step, both mass-sticking data and mass-motion data are used. The optimization constraint in Eq. (13) is applied to the former, while the Eq. (14) is applied to the latter. As the physics-based constraints are added in the time domain, this approach is different from the pre-existing approach of applying constraints using an SR3 optimizer [22]. SR3 optimizer requires the

user to specify the dependency of each coefficient appearing in the governing EOM.

While Eq. (13) yields the lower bound limit of $\hat{k}, \hat{c}, \hat{F}_f$; hence, the region above the lower bound surface is the solution, Eq. (14) provides the upper bound limit and thus the region below the upper bound surface is the solution. The lower bound and the upper bound surfaces are calculated as follows. By indicating with $(t_{\text{stop}})_j$ and $(t_{\text{slip}})_l$ the jth and lth time instants for mass-sticking and mass-motion, respectively, the lower bound $\Phi_1(\hat{k}, \hat{c})$ is obtained by using the mass-sticking condition in

$$\begin{cases} \left| \hat{c}\dot{u}(t_{\text{stop}})_j + \hat{k}u(t_{\text{stop}})_j - \hat{k}x_1(t_{\text{stop}})_j \right| = \widehat{F}_{f_j} \\ \phi_j(\hat{k}, \hat{c}) = \widehat{F}_{f_j}(\hat{k}, \hat{c}) \\ \Phi_1(\hat{k}, \hat{c}) = \max \left| \phi_j(\hat{k}, \hat{c}) \right| \end{cases} \tag{16}$$

and the upper bound $\Phi_2(\hat{k}, \hat{c})$ surfaces are obtained by using the mass-motion condition

$$\begin{cases} \left| \hat{c}\dot{u}(t_{\text{slip}})_l + \hat{k}u(t_{\text{slip}})_l - \hat{k}x_1(t_{\text{slip}})_l - \dot{x}_2(t_{\text{slip}})_l - \hat{c}x_2(t_{\text{slip}})_l \right| = \widehat{F}_{f_l} \\ \phi_l(\hat{k}, \hat{c}) = \widehat{F}_{f_l}(\hat{k}, \hat{c}) \\ \Phi_2(\hat{k}, \hat{c}) = \min \left| \phi_l(\hat{k}, \hat{c}) \right| \end{cases} \tag{17}$$

where $\widehat{F}_{f_j}$ and $\widehat{F}_{f_l}$ are the lower bound and upper bound values of friction at jth and Ith time instant, respectively. As a result, the terms $\hat{k}, \hat{c}, \hat{F}_f$, which uniquely identify the system in Eqs. (16) and (17), are not known. As both the lower bound and an upper bound represent the same dynamic system, intuitively, there should be only one triplet of $\hat{k}$, $\hat{c}$, $\hat{F}_f$, that satisfies both surfaces. However, the

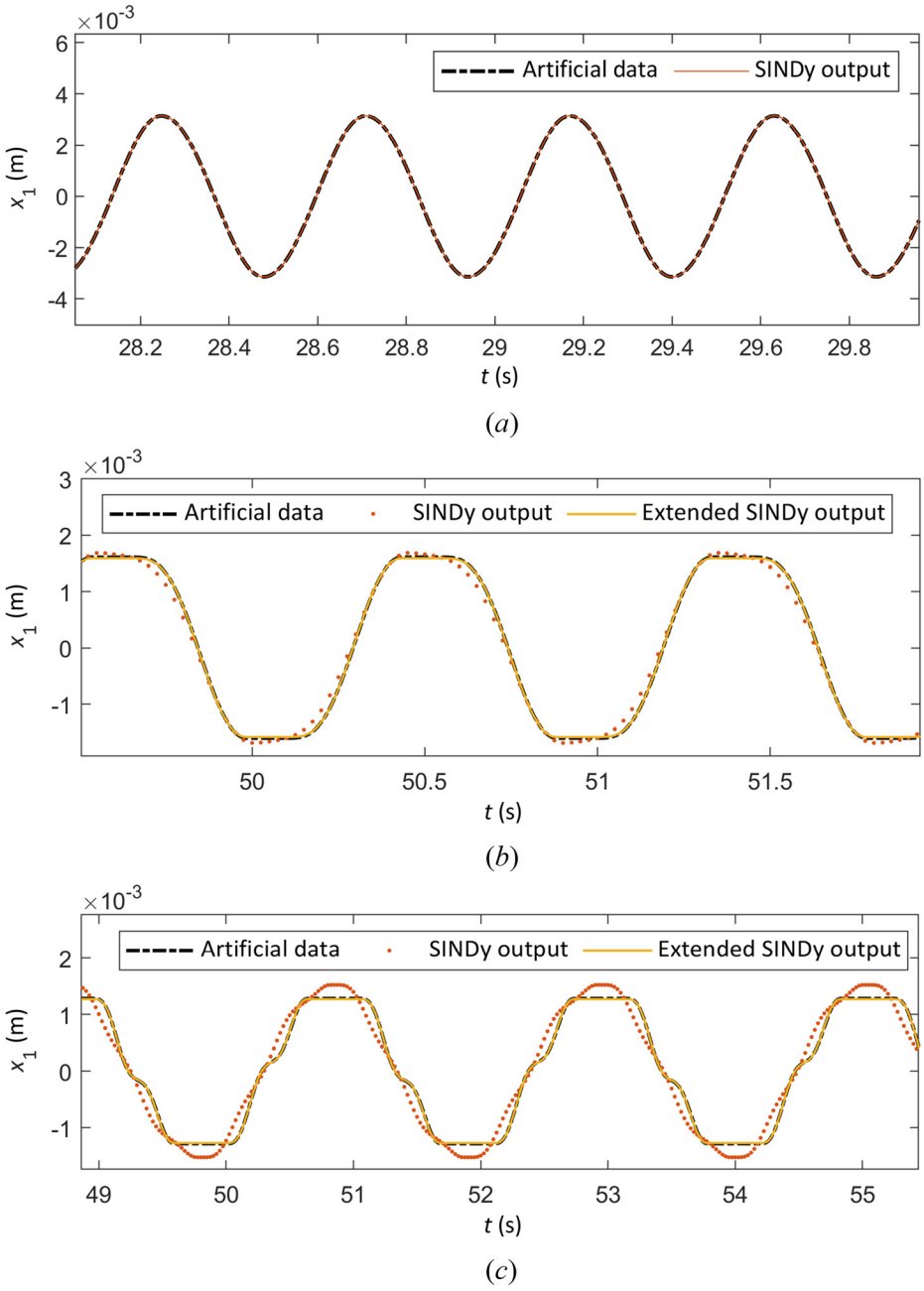

Fig. 2 Comparison between the response of the SDOF nonlinear system in the case of synthetically generated data: (*a*) continuous motion, (*b*) two-stop stick-slip motion, and (*c*) four-stop stick-slip motion

Table 4 Values of hyperparameters used in extended SINDy

Description of hyperparameters	Synthetic data	Experimental data
Threshold value for STLSq	0.03	0.03
Threshold value for SR3	0.05	0.05
Cutoff velocity for mass-sticking $\left(v_{\text{stop}}\frac{m}{s}\right)$	10^{-7}	10^{-7}
Cutoff velocity for mass-motion $\left(v_{\text{slip}}\frac{m}{s}\right)$	10^{-3}	10^{-3}
Number of datapoints considered during application of window length for smooth finite difference	35	41

generation of both surfaces is affected by numerical errors due to numerical differentiation of the measurements of position and velocity of the mass and of the input. Hence, rather than estimating the $\hat{k}$, $\hat{c}$ optimum point, it is proposed to evaluate the distance D between two surfaces perpendicular to the $\hat{k}\hat{c}-$ plane defined as

$$D(\hat{k},\hat{c}) = \left|\Phi_2(\hat{k},\hat{c}) - \Phi_1(\hat{k},\hat{c})\right| \tag{18}$$

where the distance (D) is the function of mass normalized stiffness and mass normalized viscous damping. Furthermore, the optimum triplet $\left(\hat{k}_*,\hat{c}_*,\hat{F}_{f_*}\right)$ is chosen where $D(\hat{k},\hat{c})$ is minimum, and hence, the problem is defined as

$$(\hat{k}_*,\hat{c}_*) = \underset{\hat{k},\hat{c}}{\text{argmin}}\left[D(\hat{k},\hat{c})\right] \tag{19}$$

$$\hat{F}_{f_*} = \Phi_1(\hat{k}_*,\hat{c}_*) \tag{20}$$

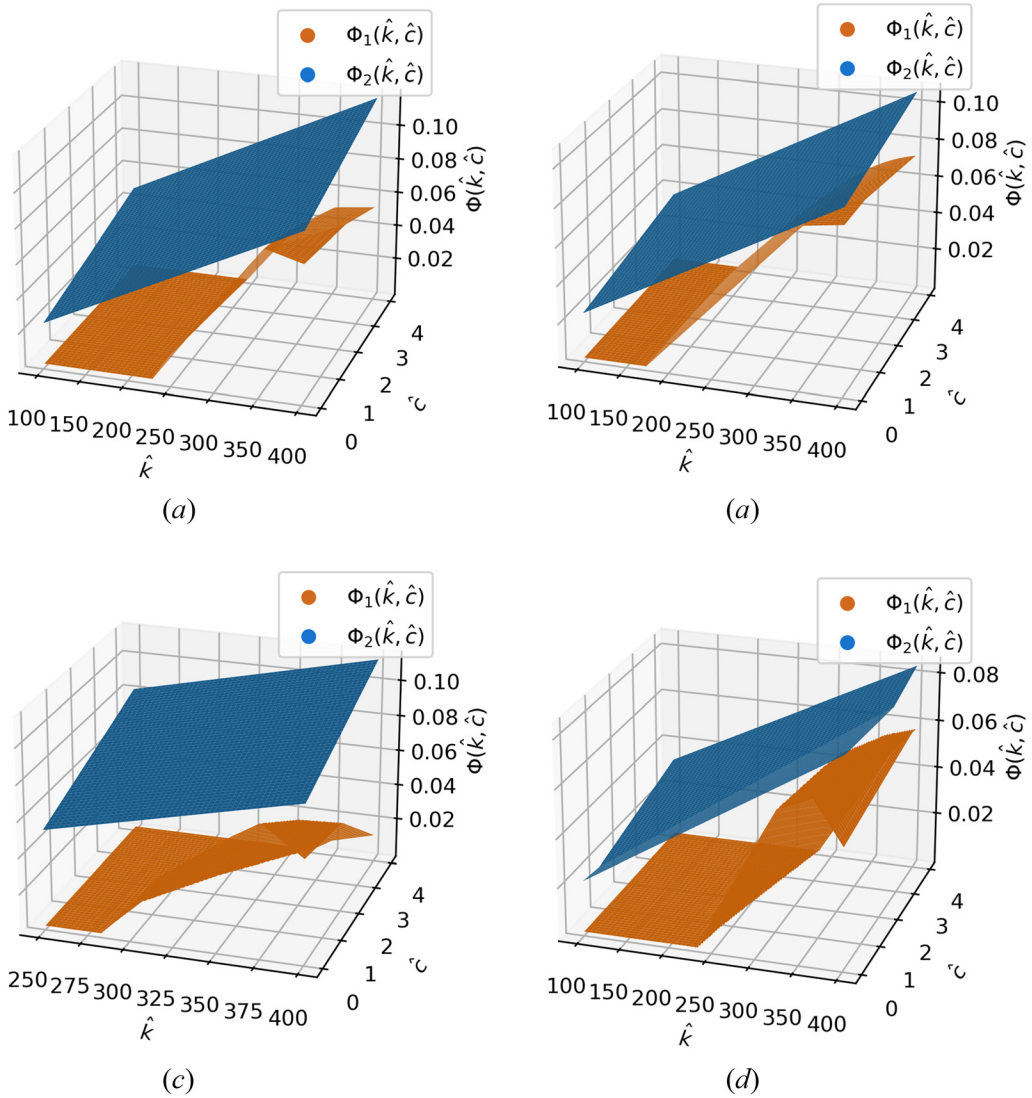

Fig. 3 Lower bound and upper bound surfaces for two-stop stick-slip synthetic model (*a*), four-stop stick-slip synthetic model (*b*), two-stop stick-slip experimental model (*c*), and four-stop stick-slip experimental model (*d*)

Table 5 Relative percentage error in parameter estimation using SINDy and extended SINDy for synthetic data

Regime	Algorithm	Relative percentage error in identification of stiffness, viscous damping, friction force magnitude (all mass-normalized) $\left(\%\frac{\Delta\hat{k}}{\hat{k}}, \%\frac{\Delta\hat{c}}{\hat{c}}, \%\frac{\Delta\widehat{F_f}}{\widehat{F_f}}\right)$
Continuous motion	SINDy	0, 23.07, 0
	Extended SINDy	Converges to SINDy
Two-stop stick-slip motion	SINDy	6.19, 623.07, 82.35
	Extended SINDy	0.84, 23.07, 5.88
Four-stop stick-slip motion	SINDy	9.82, 530.7, 70.58
	Extended SINDy	1.15, 38.46, 2.35

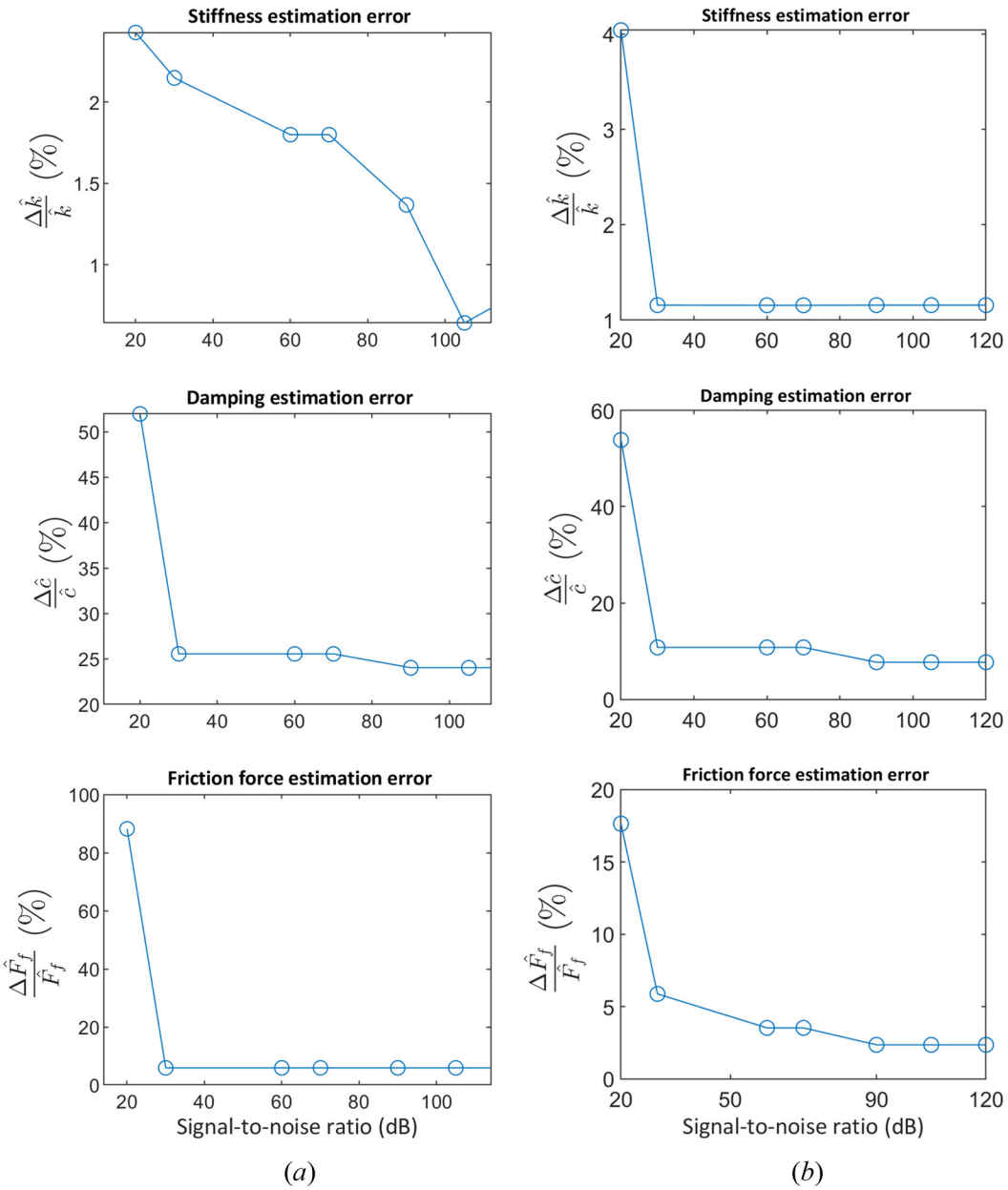

Fig. 4 Error in estimation of mass normalized stiffness, damping, and magnitude of friction force using extended SINDy for two-stop stick-slip motion (*a*) and four-stop stick-slip motion and (*b*) in presence of different levels of noise

Table 6 Conversion between standard deviation and signal-to-noise ratio

Standard deviation (σ) mm	Signal-to-noise ratio (dB)
1.4×10^{-2}	20
1.4×10^{-3}	30
1.4×10^{-6}	60
1.4×10^{-7}	70
1.4×10^{-9}	90
1.4×10^{-10}	105
1.4×10^{-12}	120

The optimum system parameters are then updated in the EOM found in step 2 of the extended SINDy. The accuracy of the identification of the optimum parameters is dependent on the noise levels in the measurement, and the window length selected to carry out the numerical differentiation of the input and output measurements. The accuracy of the numerical differentiation is also dependent on the presence of abrupt changes in the time domain caused by the nonsmooth response due to stick-slip phenomena. In particular, it is expected to observe an accuracy reduction as the number of stops per cycle in the stick–slip motion increases. All of the above will affect the generation of the upper bound and lower bound surfaces and consequently the identification error on each term of the EOM. The computational cost of this step is negligible, since it requires evaluating over a grid of k,c parameters the values of friction force according to Eqs. (13) and (14), rather than carrying out the full nonlinear analyses for each grid point. This means that the optimization in Eq. (19) is carried out explicitly having evaluated the objective function at every point of the grid. This proposed methodology is applied to the stick–slip motion with two-stops as well as four-stops.

4 Synthetic Model Case Study

Consider a SDOF oscillator with Coulomb friction contact subject to a harmonic excitation as represented in Eq. (11) and Fig. 1. The physical properties of the system are stated in Table 1. The base is excited at different frequencies to obtain continuous as well as stick-slip motion. These frequencies are mentioned in Table 2. The amplitude of base excitation is 0.0015 m. The synthetic data is generated by solving Eq. (11) with ode45 in MATLAB [20] with explicit event conditions. Both input and output datasets are then used to investigate the identification of the system parameters $(\hat{k}_*, \hat{c}_*, \hat{F}_{f_*})$ and the governing EOM with the extended SINDy. The hyperparameters used for the extended SINDy are specified in Table 4. The results obtained by using extended SINDy for various noise levels are then compared in terms of root-mean-square error (RMSE) and in terms of the relative percentage error in the estimate of the coefficients of the governing EOM to those yielded by SINDy and to their true values (as specified in Table 1). Indicating with $x_1(t)$ the synthetic data, with $[x_1(t)]_*$ the solution of the governing EOM obtained with SINDy, and with $[x_1(t)]_{**}$ the response obtained with the extended SINDy, two RMSEs can be considered

$$\mathrm{RMSE}_* = \sqrt{\sum_{i=1}^{i=N} \frac{\{x_1(t_i) - [x_1(t_i)]_*\}^2}{N}} \tag{21}$$

$$\mathrm{RMSE}_{**} = \sqrt{\sum_{i=1}^{i=N} \frac{\{x_1(t_i) - [x_1(t_i)]_{**}\}^2}{N}} \tag{22}$$

4.1 Results of System Identification of Synthetic Model With No Noise Contamination. The extended SINDy algorithm converges to the SINDy [10] algorithm in the case of continuous motion as the stick–slip time constraints for the stops are not activated. From Table 3, it is possible to observe that the system identification is accurate with a very low value of RMSE_{**}. The displacement response obtained with the extended SINDy algorithm and with SINDY is compared to the synthetic data in Fig. 2. It is possible to observe a very good agreement between the extended SINDy and the synthetic data, while the accuracy of SINDy is affected by the number of stops per cycle during stick–slip. It is also important to discuss the upper bound and lower bound surfaces (see Eqs. (16) and (17))). From Fig. 3, it is possible to observe that they do not intersect each other at one unique point due to the errors arising from numerical differentiation of $x_1(t)$ and $x_2(t)$. The relative percentage error in estimation of stiffness, viscous damping, and friction force magnitude (all mass-normalized) is reported in Table 5 . It is possible to observe that as the number of stops increases, the extended SINDy displays a much lower relative percentage error compared to SINDy.

4.2 Effect of Noise on Synthetic Model Case Study. The synthetic data are contaminated with different signal-to-noise ratio (SNR) levels to evaluate the extent of applicability of extended SINDy algorithm. This is done by using the random.normal function

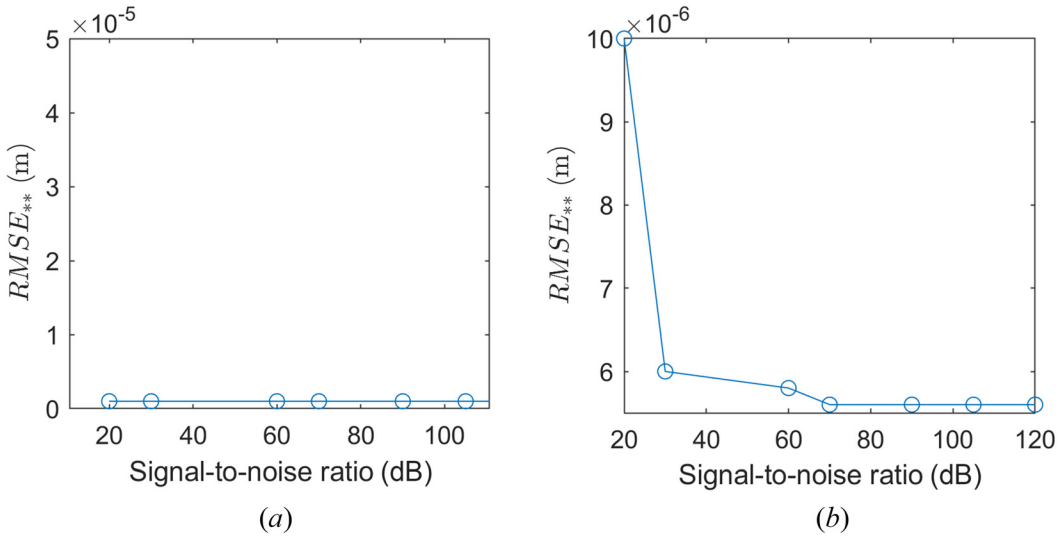

Fig. 5 Effect of noise on RMSE using extended SINDy algorithm for two-stop stick-slip motion (*a*) and four-stop stick-slip motion (*b*)

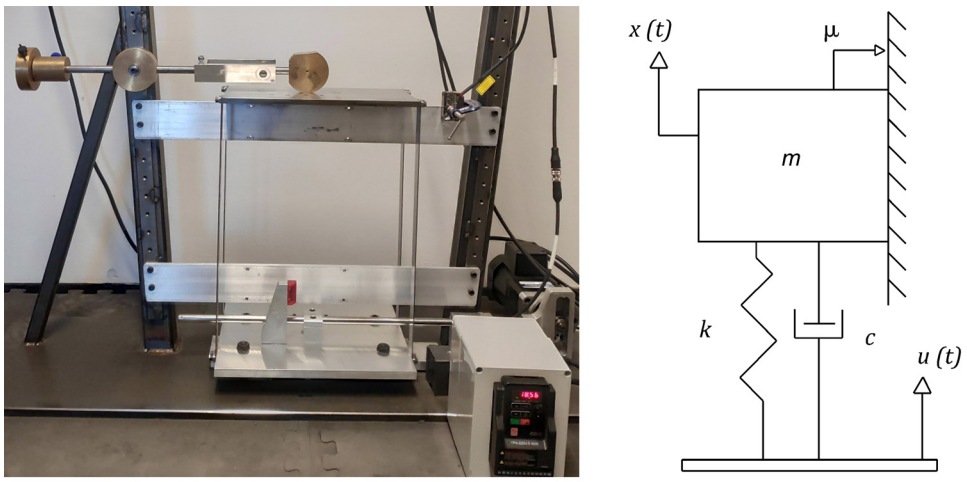

Fig. 6 SDOF dynamic system with friction as nonlinearity: (*a*) experimental setup of a SDoF with a friction contact obtained with a counter-weight system mounted on a fixed wall subject to a harmonic-base excitation and (*b*) schematic representation of SDoF with friction contact

from the NumPy library of Python with zero mean. The standard deviation of noise and the corresponding SNR levels are reported in Table 6. The effect of noise on dynamic system parameter estimation and RMSE is reported in Figs. 4 and 5. It is observed that below the SNR of 20 dB, the SINDy algorithm fails to identify the functional form of the EOM, therefore affecting the step 2 of the extended SINDy. Nonetheless, it is observed that the extended SINDy yields a lower RMSE. Above the SNR of 20 dB, the effect of noise on parameter estimation and RMSE is found within an acceptable range.

5 Experimental Model Case Study

The performance of the extended SINDy is further evaluated by considering an experimental case study, which involves a single storey frame structure with a Coulomb friction contact excited via base excitation.

5.1 Test Rig and Mechanical Model. The single-storey frame is shown in Fig. 6, and it has been used in Ref. [19]. This structure consists of an aluminum base plate connected to an electric motor via a scotch-yoke mechanism. Four thin steel bars are used to connect via bolts this base plate to a steel top plate that represents the mass of the equivalent SDOF. The base plate is excited by using an approximately harmonic excitations generated by the electric motor. A brass disk mounted on a bar pinned to the external frame is used to produce a friction contact on the top plate. The friction force is proportional to the weight of the brass disk, and it can be adjusted by using a counterweight system. The EOM of the experimental system corresponds to Eq. (12) with parameters as specified in Table 1—these were calculated by using free vibration tests on the experimental system with and without friction (as described in Ref. [19]). More details about the experimental system can be found in Ref. [19]. The parameter space investigated is such that the Coulomb friction model provides a good approximation of the friction force as shown in Ref. [23]. For the experimental data, the base excitation frequencies are given in Table 2, and the amplitude of base excitation is 0.0015 m.

5.2 Identification of the Governing Equation and Results. The hyperparameters used in extended SINDy are illustrated in Table 4. From Table 7 it can be observed that the estimated values of $\hat{k}_*$, $\hat{c}_*$, $\hat{F}_{f_*}$ obtained with the extended SINDy provide a good approximation of terms specified in Table 1, improving the accuracy of SINDy. However, compared to the numerical simulations, these results are overall less accurate. This is because the data of $x_2(\boldsymbol{t})$ and $\dot{x}_2(\boldsymbol{t})$ are affected by the nonideal harmonic excitation, other sources of the dissipation in the experimental setup not accounted for in the

Table 7 Results of system identification using experimental data

Regime	Algorithm	Equation identified	RMSE (10^{-4}m)
Continuous motion	SINDy	$\dot{x}_1 = 0.95x_2$ $\dot{x}_2 = -397.66x_1 - 0.15x_2 + 392.56u - 0.69\dot{u} - 0.031\text{sgn}(x_2)$	10.1
	Extended SINDy	Converges to SINDy	—
Two-stop stick-slip motion	SINDy	$\dot{x}_1 = 0.97x_2$ $\dot{x}_2 = -362.56x_1 - 0.731x_2 + 352.1u + 1.2\dot{u} - 0.015\text{sgn}(x_2)$	2.8
	Extended SINDy	$\dot{x}_1 = 0.97x_2$ $\dot{x}_2 = -365.48x_1 - 0.04x_2 + 365.48u + 0.04\dot{u} - 0.08\text{sgn}(x_2)$	1.35
Four-stop stick-slip motion	SINDy	$\dot{x}_1 = 0.97x_2$ $\dot{x}_2 = -371.48x_1 - 1.02x_2 + 369.7u + 1.5\dot{u} - 0.002\text{sgn}(x_2)$	5.4
	Extended SINDy	$\dot{x}_1 = 0.97x_2$ $\dot{x}_2 = -364.56x_1 - 0.08x_2 + 364.56u + 0.08\dot{u} - 0.065\text{sgn}(x_2)$	1.52

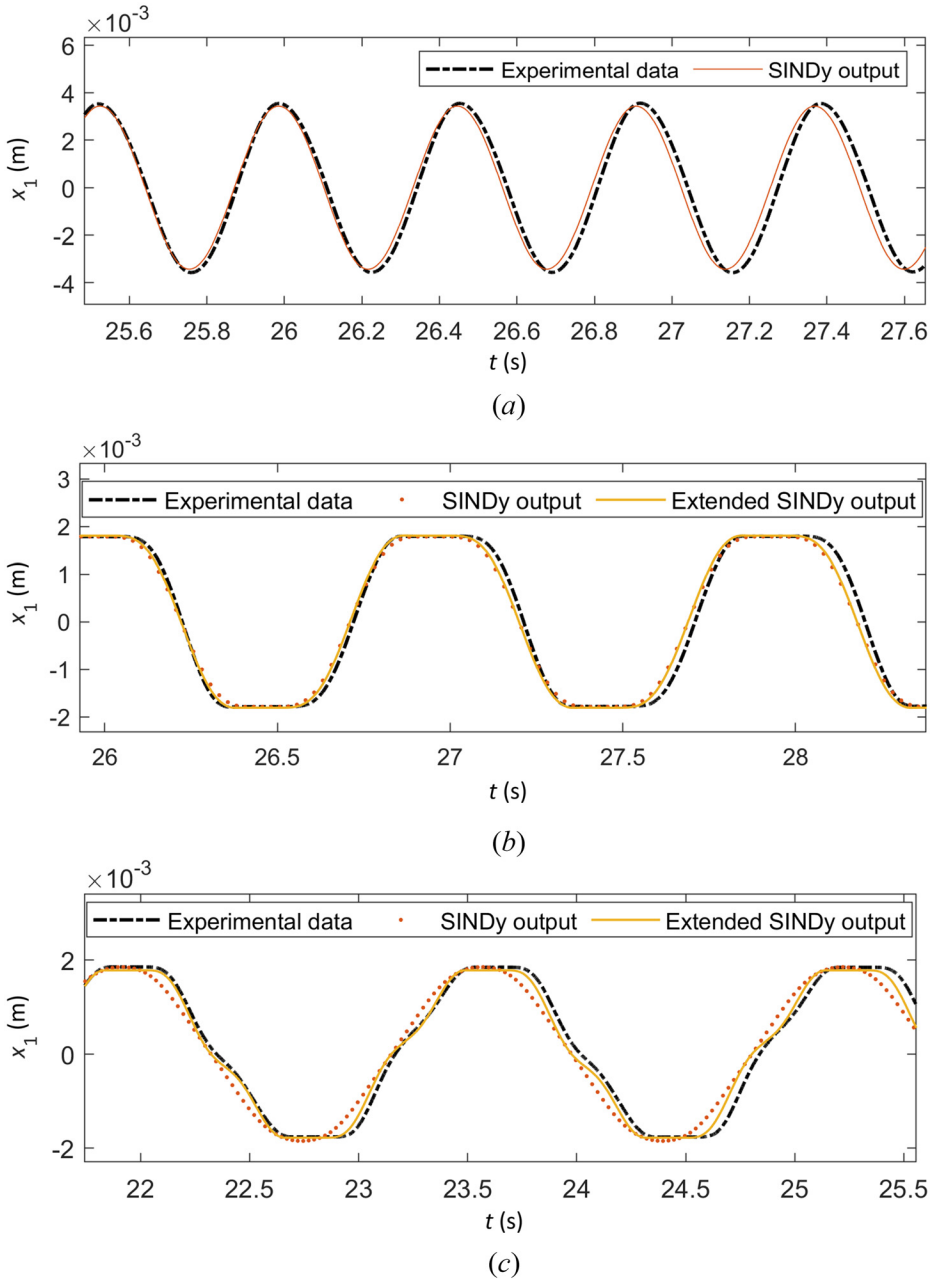

Fig. 7 Comparison between the response of the SDOF nonlinear system in the case of experimentally generated data: (*a*) continuous motion, (*b*) two-stop stick-slip motion, and (*c*) four-stop stick-slip motion

Table 8 Relative percentage error in parameter estimation using SINDy and extended SINDy for experimental data

Regime	Algorithm	Relative percentage *error* in identification of stiffness, viscous damping, friction force magnitude (all mass-normalized) $\left(\%\frac{\Delta\hat{k}}{\hat{k}}, \%\frac{\Delta\hat{c}}{\hat{c}}, \%\frac{\Delta\hat{F}_f}{\hat{F}_f}\right)$
Continuous motion	SINDy	10.86, 130.76, 63.52
	Extended SINDy	Converges to SINDy
Two-stop stick-slip motion	SINDy	1.074, 1024.6, 82.35
	Extended SINDy	1.88, 38.46, 5.88
Four-stop stick-slip motion	SINDy	3.56, 1469.23, 97.64
	Extended SINDy	1.63, 23.07, 23.52

mathematical model and because of additional numerical errors caused by the numerical differentiation. The difference between the results yielded by the SINDy and the extended SINDy is not obvious in the case of two-stop stick-slip motion reported in Fig. 7. However, a difference can be observed in terms of RMSE from Table 7. Further, from Fig. 7, it is possible to observe a notable difference between the results yielded by SINDy and extended SINDy for four-stop stick-slip motion. The improvement in parameter identification when using the extended SINDy can be further observed in Table 8.

6 Conclusion

An extended SINDy algorithm has been proposed for identifying the governing EOM of a SDOF system with friction contact subject to a harmonic excitation. It is shown that the existing SINDy approach is unable to accurately identify the epistemic uncertainty of the system parameters such as the stiffness, viscous damping, and friction force (all mass normalized) of the dynamic system. The extended SINDy overcomes these limitations by using the SINDy algorithm on part of the data to evaluate the functional form of the governing EOM and by incorporating physics knowledge by using stick and slip temporal constraints. The last step is implemented by employing a constrained optimization strategy. The proposed extended SINDy algorithm is applied to the data obtained from two dynamic systems, namely, a synthetic SDOF oscillator with friction contact subject to a harmonic excitation and an experimental setup representing a SDOF dynamic system with steel to brass contact subject to an approximately harmonic base input. A good agreement was found between the estimated system parameters and the actual system parameters of both the above-stated systems.

The main advantage of the extended SINDy algorithm over existing data-driven algorithms is that it can explicitly incorporate the physics constraints in the time domain. The output is in the form of an EOM and hence can be used to interpret the uncertain system parameters like stiffness, viscous damping and nonlinear friction force, all normalized with mass. Leveraging on the SINDy algorithm, the extended SINDy algorithm can accurately estimate the system parameters for various noise levels. It has been observed that an improved parameter estimate is obtained when using a dataset which includes the transient response (measured from zero initial conditions) and the steady-state response caused by a sinusoidal load.

Although the current investigations have been limited to a nonsmooth nonlinearity caused by a friction contact, the proposed approach can be generally applied to SDOF dynamic systems with discontinuous nonlinearity causing the system to show different motion behavior which can be explicitly identified with physics constraints. Current investigations are exploring the applicability of the extended SINDy algorithm to the multi-degrees-of-freedom (MDOF) dynamic system with single and multiple friction contacts and to a random external excitation.

The proposed methodology can be used in identifying the model parameters and identifying the governing EOM of a SDOF dynamic system in laboratory conditions. Using the obtained EOM, a representative virtual model of the dynamic system is identified. This enables the virtual investigations of the behavior of such system under a broad range of loading conditions that might not be possible to reproduce in laboratory conditions because of cost or time constraints. The proposed approach is a first step toward the real-time identification of nonlinearity of structural joints in operating conditions. It is worth mentioning that the implementation of more advanced numerical differentiation schemes might improve the accuracy in estimating the lower bound and upper bound surfaces. This will further improve in accurately estimating the system parameters $\hat{k}_*$, $\hat{c}_*$, $\hat{F}_{f_*}$.

Acknowledgment

The authors would like to acknowledge helpful discussion with L. Marino and with C. Lathourakis.

Data Availability Statement

The datasets generated and supporting the findings of this article are obtainable from the corresponding author upon reasonable request.

Nomenclature

ARX = auto-regressive with eXogenous input
EOM = equation of motion
ML = machine learning
MDOF = multi-degrees-of-freedom
NARMAX = nonlinear auto-regressive moving-average with eXogenous inputs model
NARX = nonlinear auto-regressive with eXogenous
RMSE = root-mean-square error
SDOF = single degree-of-freedom
SINDy = sparse identification of nonlinear dynamics
SNR = signal-to-noise ratio
SR3 = sparse relaxed regularized regression

References

[1] Bouc, R., 1994, "The Power Spectral Density of Response for a Strongly Non-Linear Random Oscillator," J. Sound Vib., **175**(3), pp. 317–331.
[2] Caughey, T. K., 1963, "Equivalent Linearization Techniques," J. Acoust. Soc. Am., **35**(11), pp. 1706–1711.
[3] Caughey, T. K., 1960, "Random Excitation of a System With Bilinear Hysteresis," ASME J. Appl. Mech., **27**(4), pp. 649–652.
[4] Caughey, T. K., 1959, "Response of Van Der Pol's Oscillator to Random Excitation," ASME J. Appl. Mech., **26**(3), pp. 345–348.
[5] Soize, C., 1993, "Stochastic Linearization Method With Random Parameters and Power Spectral Density Calculation," Paper Presented at the Sixth International Conference on Structural Safety and Reliability (ICOSSAR'93), Innsbruck, Austria, Dec., pp. 143–152.
[6] Leontaritis, I. J., and Billings, S. A., 1985, "Input-Output Parametric Models for Non-Linear Systems Part I: Deterministic Non-Linear Systems," Int. J. Control, **41**(2), pp. 303–328.
[7] Leontaritis, I. J., and Billings, S. A., 1985, "Input-Output Parametric Models for Non-Linear Systems Part II: Stochastic Non-Linear Systems," Int. J. Control, **41**(2), pp. 329–344.
[8] Billings, S. A., Chen, S., and Backhouse, R. J., 1989, "The Identification of Linear and Non-Linear Models of a Turbocharged Automotive Diesel Engine," Mech. Syst. Signal Process., **3**(2), pp. 123–142.
[9] Kerschen, G., Worden, K., Vakakis, A. F., and Golinval, J.-C., 2006, "Past, Present and Future of Nonlinear System Identification in Structural Dynamics," Mech. Syst. Signal Process., **20**(3), pp. 505–592.
[10] Brunton, S. L., Proctor, J. L., and Kutz, J. N., 2016, "Discovering Governing Equations From Data by Sparse Identification of Nonlinear Dynamical Systems," Proc. Nat. Acad. Sci., **113**(15), pp. 3932–3937.
[11] de Silva, B. M., Champion, K., Quade, M., Loiseau, J.-C., Kutz, J. N., and Brunton, S. L., 2020, "PySINDy: A Python Package for the Sparse Identification of Nonlinear Dynamics From Data," preprint arXiv:2004.08424.
[12] Fasel, U., Kaiser, E., Kutz, J. N., Brunton, B. W., and Brunton, S. L., 2021, "Sindy With Control: A Tutorial," Paper Presented at the 60th IEEE Conference on Decision and Control (CDC), Austin, TX, Dec. 14-17, pp. 16–21.
[13] Hoffmann, M., Fröhner, C., and Noé, F., 2019, "Reactive Sindy: Discovering Governing Reactions From Concentration Data," J. Chem. Phys., **150**(2), p. 025101.
[14] Lakshminarayana, S., Sthapit, S., and Maple, C., 2022, "Application of Physics-Informed Machine Learning Techniques for Power Grid Parameter Estimation," Sustainability, **14**(4), p. 2051.
[15] Sandoz, A., Ducret, V., Gottwald, G. A., Vilmart, G., and Perron, K., 2023, "Sindy for Delay-Differential Equations: Application to Model Bacterial Zinc Response," Proc. R. Soc. A, **479**(2269), p. 20220556.
[16] Huang, S.-C., Chen, H.-W., and Tien, M.-H., 2023, "Predicting Nonlinear Modal Properties by Measuring Free Vibration Responses," ASME J. Comput. Nonlinear Dyn., **18**(4), p. 041005.
[17] Didonna, M., Stender, M., Papangelo, A., Fontanela, F., Ciavarella, M., and Hoffmann, N., 2019, "Reconstruction of Governing Equations From Vibration Measurements for Geometrically Nonlinear Systems," Lubricants, **7**(8), p. 64.
[18] Hilborn, R. C., 2000, *Chaos and Nonlinear Dynamics: An Introduction for Scientists and Engineers*, Oxford University Press, Oxford, UK.
[19] Marino, L., and Cicirello, A., 2020, "Experimental Investigation of a Single-Degree-of-Freedom System With Coulomb Friction," Nonlinear Dyn., **99**(3), pp. 1781–1799.
[20] The MathWorks Inc., 2020, "MATLAB, Version 9.9.0.1857802 (R2020b)," The Mathworks Inc., Natick, MA.
[21] Marino, L., Cicirello, A., and Hills, D. A., 2019, "Displacement Transmisibiltiy of a Coulomb Friction Oscillator Subject to Joined Base-Wall Motion," Nonlinear Dyn., **98**(4), pp. 2595–2612.
[22] Zheng, P., Askham, T., Brunton, S. L., Kutz, J. N., and Aravkin, A. Y., 2019, "A Unified Framework for Sparse Relaxed Regularized Regression: Sr3," IEEE Access, **7**, pp. 1404–1423.
[23] Cabboi, A., Marino, L., and Cicirello, A., 2022, "A Comparative Study Between Amontons–Coulomb and Dieterich–Ruina Friction Laws for the Cyclic Response of a Single Degree of Freedom System," Eur. J. Mech.-A/Solids, **96**, p. 104737.